Desalination and Water Treatment
www.deswater.com

doi: 10.1080/19443994.2015.1110052

57 (2016) 20738–20748
September

Taylor & Francis
Taylor & Francis Group

Reverse osmosis membranes for water desalination based on cellulose acetate extracted from Egyptian rice straw

Sh. Ebrahim[a,*], A. Morsy[a,b], E. Kenawy[c], T. Abdel-Fattah[d], S. Kandil[a]

[a]*Materials Science Department, Institute of Graduate Studies & Research, Alexandria University, 163 Horreya Avenue, El-Shatby, Alexandria 21526, Egypt, Tel. +20 124879137; Fax: +20 34295007; email: shebrahim@alex-igsr.edu.eg (S. Ebrahim), Tel. +20 1211184883; Fax: +20 034770012; email: ashrafchamist@yahoo.com (A. Morsy), Tel. +20 1003400746; Fax: +20 34295007; email: s.kandil@usa.net (S. Kandil)*
[b]*Department of Chemistry, Egyptian Petrochemicals Company, Alexandria, Egypt*
[c]*Faculty of Science, Chemistry Department, Tanta University, Tanta, Egypt, Tel. +20 1222372276; Fax: +20 403350804; email: ekenawy@science.tanta.edu.eg*
[d]*Applied Research Center, Thomas Jefferson National Accelerator Facility and Department of Molecular Biology, and Chemistry, Christopher Newport University, Newport News, VA 23606, USA, Tel. +1 757 594 7606; Fax: +1 757 594 7209; email: fattah@cnu.edu*

Received 19 July 2015; Accepted 13 October 2015

ABSTRACT

Cellulose diacetate (CDA) and cellulose triacetate (CTA) were extracted from Egyptian rice straw. Reverse osmosis (RO) membranes were prepared from this CDA using phase inversion technique. The structural, crystalline, morphological, and hydrophilic properties of the prepared membranes were characterized by Fourier transform infrared spectroscopy, proton nuclear magnetic resonance (^{1}HNMR), X-ray diffraction (XRD), scanning electron microscopy (SEM), and contact angle measurements, respectively. The NMR spectra revealed a degree of substitution of 2.8 for CTA and 1.75 for CDA. The values of water flux and salt rejection for CA-RO membrane without annealing, tested in 10,000 ppm NaCl, were 7.1 L/m^2 h and 87.4%, respectively, while the water flux of 4.76 L/m^2 h and a salt rejection of 93.3% were obtained for the annealed CA-RO membrane at 14 bar. The annealed CA-RO membranes showed an asymmetric structure with ridge-and-valley on the top layer and macrovoid structures in the support layer as revealed by SEM. The CA-RO membranes grafted with 15 wt% of 2-acrylamidopropane-2-methyl sulfonic acid produced a salt rejection of 93.5% and a water flux of 8.3 L/m^2 h. It was concluded that both the annealing and grafting processes enhanced the performance of the CA-RO membranes.

Keywords: Cellulose; Cellulose acetate; Reverse osmosis; Membrane; Desalination

1. Introduction

Egypt is facing various serious problems: pollution coming from rice straw and further agriculture wastes, agriculture drainage, and water scarcity. Innovative and radical approaches, methods, and materials should address these pressing problems. In Egypt, rice cultivation produces large amounts of rice straw as a residue. Assuming that about 20% are used for other purposes, about 2.8 Mt are left on the fields to be

---

*Corresponding author.

burnt in the harvesting season within a period of 30 d to get rid of the leftover debris. The resulting emission seriously pollutes the air and produces a "Black Cloud" [1]. Cellulose isolated from rice straw contains about 45–70% complex carbohydrates (cellulose and hemicellulose). It can be pretreated with dilute alkaline and acidic solutions successively; then it can be further transformed into cellulose acetate in the presence of acetic anhydride and phosphotungstic acid. This cheap natural polymer, with its hydrophilic properties, is an important material for different applications [2–4]. Cellulose acetate can be used in seawater desalination where reverse osmosis (RO) process is considered one of the most effective techniques due to its high potable water quality [5]. The cellulose acetate membranes have now been replaced with thin film composite membranes, however, cellulose acetate membranes still keep with a small fraction of the industry. They are easy to make, mechanically tough, and resistant to degradation by chlorine and other oxidants, a problem with thin-film composite membranes. Cellulose acetate membranes can tolerate up to 1 ppm chlorine, so chlorination can be used to sterilize the feed water, a major advantage with feed streams having a significant bacterial loading. The water and salt permeability of cellulose acetate membranes is sensitive to the degree of acetylation of the polymer used to make the membrane [6–8].

The aim of this work is to prepare cellulose diacetate (CDA) and cellulose triacetate (CTA) from Egyptian rice straw using acetylation of the extracted cellulose. Then CA-RO membranes were prepared using phase inversion technique from the CDA produced from the acetylation of the extracted cellulose. The performance of these membranes is dependent on its chemical structure and physical properties. Therefore, it is important to fully characterize the produced membranes, its structure, morphology, and hydrophilicity. Fourier transform infrared (FTIR), ^{1}HNMR, X-ray diffraction (XRD), scanning electron microscopy (SEM), and contact angle measurements were performed on the prepared CA-RO membranes. Furthermore, the effect of annealing and grafting using 2-acrylamidopropane-2-methyl sulfonic acid (AMPSA) on water flux and salt rejection of CA-RO membranes was investigated using cross-flow RO testing unit.

2. Materials and methods

2.1. Materials

Acetic anhydride, acetone, magnesium perchlorate, sodium hydroxide pellets, and sulfuric acid were obtained from Fisher Scientific. Glacial acetic acid was purchased from Fluka chemika. Cellulose acetate (weight-average molecular weight 100,000 g/mol, 39.8 wt% acetyl) and chloroform were received from Aldrich. 1,4-Dioxane was supplied by Panreac Quimica S.A (Barcelona, Spain). Methanol was used as received from Labsolve (Lisbon, Portugal). Egyptian rice straw was obtained from the local farms.

2.2. Extraction of cellulose from Egyptian rice straw

Egyptian rice straw was washed with hot water and NaOH (15%) to remove lignocellulose. The pretreated rice straw was acidified to pH 5.0 before using as a starting material; the solids were separated from the liquids, washed once with three volumes of water, and dried in an oven at 60˚C.

2.3. Acetylation of cellulose

Milled rice straw (2.0 g) was first dried, and mixed with acetic acid (35 mL) in a 250-mL beaker, and was covered with a glass watch. The mixture was placed in a water bath and its temperature was maintained at 50–55˚C for 30 min with continuous stirring. An acetylating mixture consisting of acetic anhydride (10 mL) and concentrated sulfuric acid (0.4 mL) was added to the above reaction mixture. The reaction mixture was then kept in a water bath for one hour at 50–55˚C with continuous stirring until a clear solution was obtained. This mixture was then divided into two equal parts. The first portion (22.7 mL) was used in preparing CTA by carefully pouring it into a large volume of water (500 mL) with stirring. CTA was formed as a precipitate. This precipitate was filtered, and washed to neutrality, and was dried in air. To the second portion (22.7 mL) of the mixture, acetic acid (12.0 mL) and water (3.5 mL) were added together with stirring to avoid precipitation. The mixture was allowed to stand for 1 h at 50–55˚C. This mixture was poured into a large volume of water and the CDA precipitate was formed. This was filtered through a Buckner funnel, and washed to neutrality, and was dried in air [9]. Fig. 1 shows the schematic diagram of the preparation steps of cellulose acetate from rice straw.

2.4. Preparation of pristine and grafted CA-RO membranes

Asymmetric CA-RO membranes were prepared by the phase inversion method. The CA-RO membranes were prepared using dioxane (27 wt%), acetone (13.5 wt%), and acetic acid (5 wt%) as solvents for CA (8.45 wt%), while methanol (10.7 wt%) was used as a non-solvent [10]. The membranes were obtained

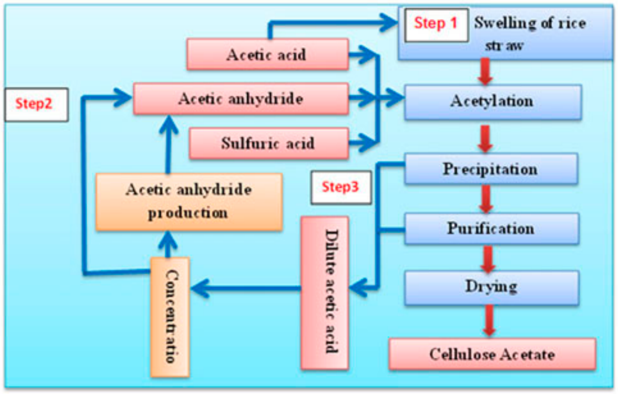

Fig. 1. Schematic diagram of the preparation steps of cellulose acetate from rice straw.

through the spreading of the solution at room temperature on a glass plate with a ruler, at a constant speed (10 mm/s) where the thickness was previously selected (250 μm), using an automatic film applicator. After evaporation of the solvent (in 60 s), the polymeric film that precipitated on the glass was immersed in an ice water bath for 15 min. After the cellulose acetate membrane was formed, the film was placed in a water bath around 4˚C for 2 h. The last step of this process was annealing that took place for 10 min at 80–85˚C. For the preparation of the grafted CA-RO membranes, sodium hydroxide (0.04%) was poured on the top surface of the CA-RO membranes for 5 min to induce partial deacetylation of the CA-RO membrane. After washing the membranes several times by deionized water, potassium persulfate (1.5 wt %) was added dropwise onto the CA-RO membrane top surface for 10 min to form a free radical. Different weight percentages (15 and 20) of AMPSA were poured onto the CA-RO membrane surface for 10 min at room temperature to allow the grafting reaction to take place. The functionalized CA-RO membranes were washed again by deionized water for several times to remove the unreacted chemicals. Finally, the membranes were thermally heated at 75˚C for 30 min. Then these membranes were soaked in deionized water for 24 h.

2.5. Characterization techniques

2.5.1. DS of cellulose acetate

The distribution of the acetyl moiety among the three OH groups of AGU of cellulose acetate was calculated from the proton nuclear magnetic resonance (^{1}HNMR) spectra of a solution of cellulose ester in dimethyl sulfoxide. Nuclear magnetic resonance (JEOL GNM ECA 500) was used and the degree of substitution (DS) of cellulose acetate was calculated by integrating the area of peaks using the following equation [11]:

$$\mathrm{DS} = \frac{7 \times I_{\mathrm{acetyl}}}{3 \times I_{\mathrm{AGU}}} \tag{1}$$

where I_{acetyl} is the integration of the methyl protons of the acetyl moieties, while I_{AGU} is the integration of all the protons of anhydroglucose unit (AGU).

2.5.2. Chemical structure

FTIR spectrometer (FTIR LX 18-5255 Perkin Elmer) was used for characterizing the membranes. The spectra were recorded in the wave number range of 4,000–400 cm^{-1} for the prepared CA and CA-RO membranes. The CA samples were ground with KBr in a ratio of 1:10 in the powder form to reduce the particle size; otherwise, the large particles will scatter the IR beam and cause a slope in the baseline of the spectrum [4]. The powdered mixture was then pressed in a hydraulic press to form a translucent disk through which the beam of the spectrometer can pass.

2.5.3. Solubility test

To evaluate the solubility of the CTA and CDA, a polymer powder sample (5 mg) was added to common organic solvents such as acetone, chloroform, or a mixture of chloroform (5 mL) and methanol (9:1, v/v) and stirred thoroughly. After the mixture was stirred continuously for 24 h at room temperature, the solubility of the polymers was observed. The resulting action of each liquid on the polymer was described simply as being a solvent or a non-solvent. A solvent is the one which produced a clear solution or a slightly turbid one that could not be separated by centrifugation.

2.5.4. Crystallinity characterization

XRD scans were carried out using X-ray 7000 Schimadzu-Japan at room temperature in the Bragge angle (2θ) ranging from 10 to 80˚ to determine the degree of crystallinity. The X-ray source utilized was Cu target with settings of 30 kV and 30 mA, with a scan speed of 4 deg/min.

2.5.5. Thermal analysis

Thermal gravimetric analysis (TGA) was carried out using (TA-SDT Q600) thermal analysis system; the sample (7 mg) was placed in a platinum pan and was heated from 20 to 600°C with a heating rate of 10°C/min in N_2 atmosphere with a flow rate of 25 ml/min.

2.5.6. Hydrophilicity measurements

The contact angle of the CA-RO membranes' surfaces was measured using Rame-hart, Instrument Company, France, where drops of distilled water (2 μL) were placed on the CA-RO membrane surface (3 cm × 2 cm) using a microsyringe (Hamilton Company, Reno, NV). The contact angles were measured within 30 s after the water drops were placed. The average of five drops measured at different positions was taken as the contact angle.

2.5.7. Morphology investigation

To produce the cross-sectional, surface, and bottom images of the membrane, SEM, XL 30 JEOL, was used. The morphological images of the cross section of the CA-RO membranes were snapped under liquid nitrogen that was used to give a generally consistent and clean break of the membrane. The membranes were sputter coated with a thin film of gold and were mounted on a brass plate using double-sided adhesion tape in a lateral position. Atomic force microscopy (AFM) was recorded by attaching square samples (approx. 1 cm^2) to an AFM stub with carbon tape. AFM images were obtained in tapping mode in air with a multimode atomic force microscope, equipped with a Nanoscope IV scanning probe, at ambient temperature.

2.5.8. Membrane performance

The performance (salt rejection and water flux) of CA-RO membranes (area 42 cm^2) was evaluated using cross-flow RO unit, (CF042, Sterling, USA) with hydra pump, pressure control valve, and gage through rejection line, with variable frequency drive (SV015IG5A-4) and flow meter (F-550 USA) as shown in Fig. 2. Saline salt solutions of NaCl of 10,000 with pH 7 were used. The total dissolved salts of the permeate water were measured using pH/conductivity meter (430 portable, Jenway, England).

The performance of the membranes was evaluated by the flux (F) and salt rejection (R) values from the following equations [12,13]:

$$F = \frac{V}{A \times t \times p} \tag{2}$$

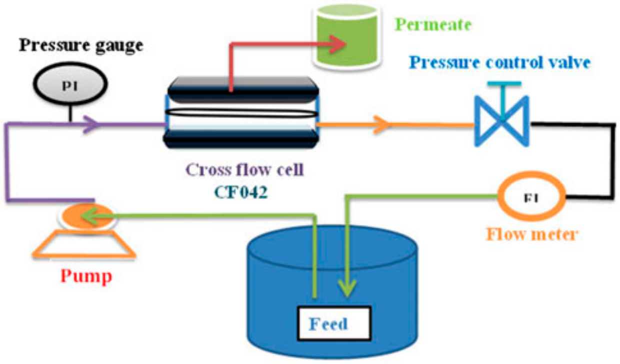

Fig. 2. Cross-flow RO test unit.

$$R = (C_o - C_{memb}) \times \frac{100}{C_o} \tag{3}$$

where V is the volume of water passing through the membrane (L), A is the membrane area (m^2), t is the time (h), and p is the pressure across the membrane (bar). C_o is the conductivity of salty water at the pressure side in the beginning of the experiment (mS) and C_{memb} is the conductivity of water that goes through the membrane (mS).

3. Results and discussion

3.1. Mechanism of acetylation of the extracted cellulose

It was found that the yield of the prepared CDA and CTA from rice straw is 50 wt%. In the first step of acetylation process, the acetic anhydride takes a proton (a hydrogen ion) from the concentrated sulfuric acid. The proton is attached to one of the lone pairs on the oxygen of cellulose which is double bonded to the carbon. This oxygen acquires a positive charge due to the transfer of this proton. The acetate groups in the acetic anhydride are easily substituted to form sulfoester groups as shown in Fig. 3. The reaction is carried out at a temperature that is less than 50°C and the cellulose triacetate is produced. Due to the hydrolysis of the cellulose in acidic media, a reduction in the DS of the cellulose has occurred. The rate of the reaction as well as the extent of cellulose degradation is dependent on the amount of acid and the reaction temperature (55°C). CTA that was produced from the previous reaction is partially hydrolyzed, which consumes the excess acid to obtain CDA. The resulting reaction from the addition of water and acetic acid to CTA is highly exothermic. As the quantity of water increases, the reverse reaction proceeds and complete hydrolysis occurs. It is not possible to obtain the

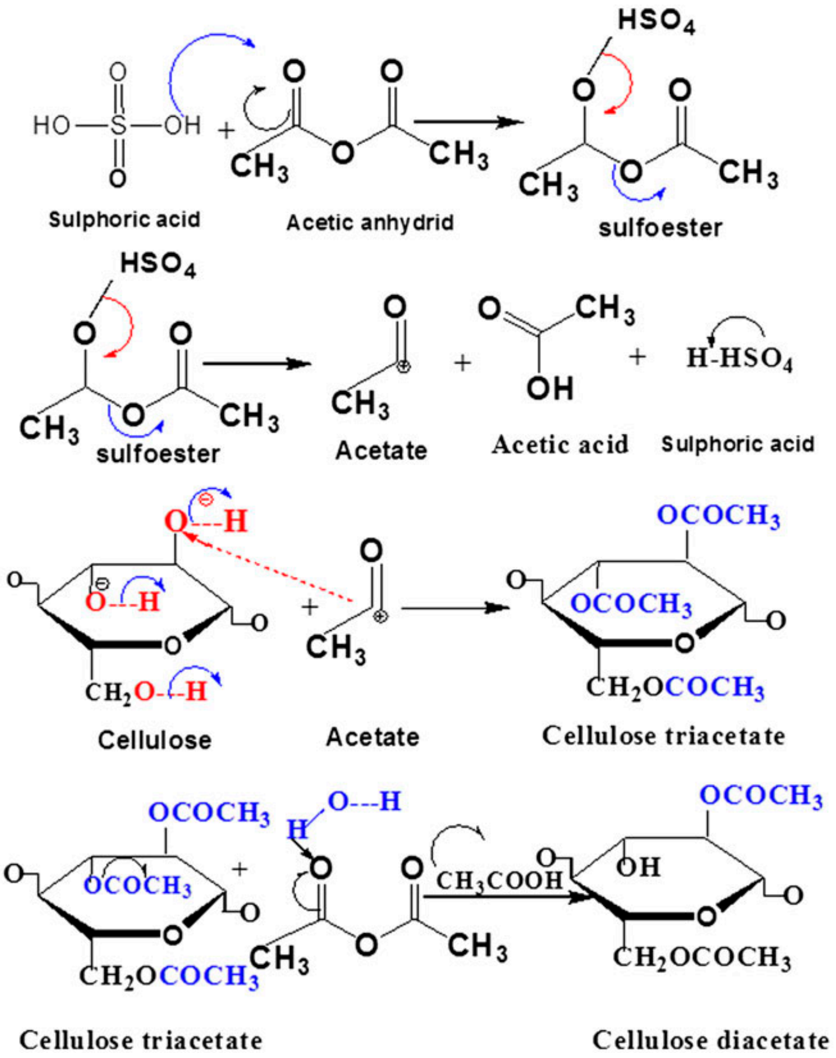

Fig. 3. Reaction mechanisms of acetylation of the extracted cellulose to obtain CTA and CDA.

doubly substituted CDA from cellulose directly via the acetylation as it is difficult to control and terminate the reaction in the CDA stage. Higher water content helps to minimize the degradation of cellulose acetate.

3.2. DS-^{1}HNMR of CA

The relative DS of the hydroxyl groups was estimated from the ratio between the peak heights or peak areas of the hydroxyl groups to the total proton areas in the NMR spectra. Generally, the integrated ratio of the seven cellulose protons resonating in the range of 3.5–5.1 ppm to the integrated absorbance of the three methyl protons of the acetyl groups resonating in the range of 1.9–2.2 ppm determines the DS of CA [14]. The ^{1}HNMR spectrum of CTA has three hydroxyl groups that have been substituted with three acetyl groups, triacetate, whereas the CDA has only two hydroxyl groups that have been substituted by acetyl groups. Fig. 4 shows the ^{1}HNMR spectrum of CTA prepared from rice straw with a DS of 2.8. ^{1}HNMR spectrum of CDA prepared from rice straw is presented in Fig. 5. The peaks of the methyl groups of the substituent acetyl groups at the region of 1.91–2.04 ppm and the ring protons' resonances arising from seven ring protons of H1-H6 in each AGU appear in the region of 3.31–5.05 ppm. The integrated value of the methyl protons is 6.0, where the integrated value of the total ring protons is set to 8.0. This indicates that DS of the CDA is 1.75 [14–16].

3.3. Structural group frequencies of the prepared CA

The FTIR spectra of the cellulose, CDA, and CTA that were extracted from rice straw were compared to the commercial or reference cellulose acetate as shown

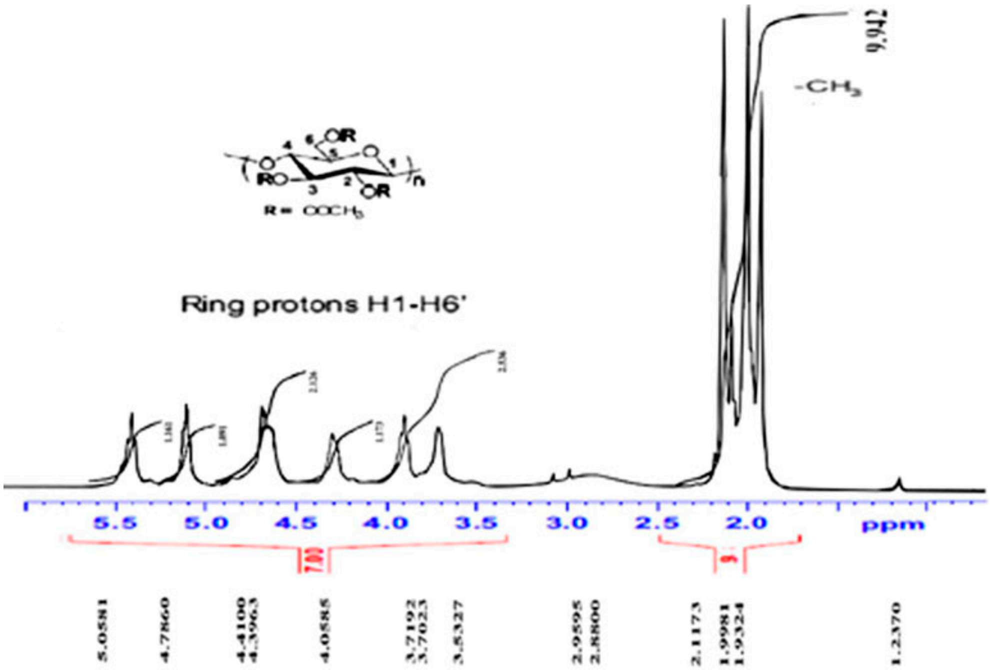

Fig. 4. ^{1}HNMR spectrum of CTA prepared from rice straw.

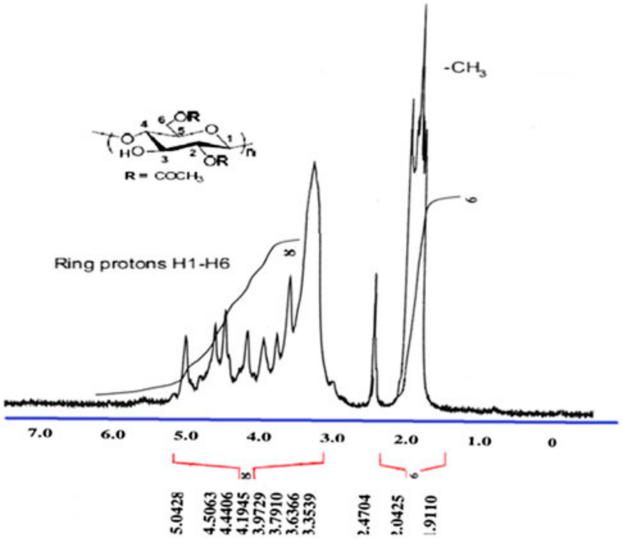

Fig. 5. ^{1}HNMR spectrum of CDA prepared from rice straw.

in Fig. 6. The extracted cellulose has a broad band at 3,448 cm^{-1} that was attributed to the stretching of the hydroxyl groups and the band at 2,950 cm^{-1} which is attributed to the CH$_3$ stretching. In addition, the H–O–H bending group of the absorbed cellulose water appeared at 1,674 cm^{-1}. The broad peak at 1,404 cm^{-1} corresponded to the C–H bending, while the band at 1,050 cm^{-1} corresponded to the stretching modes of

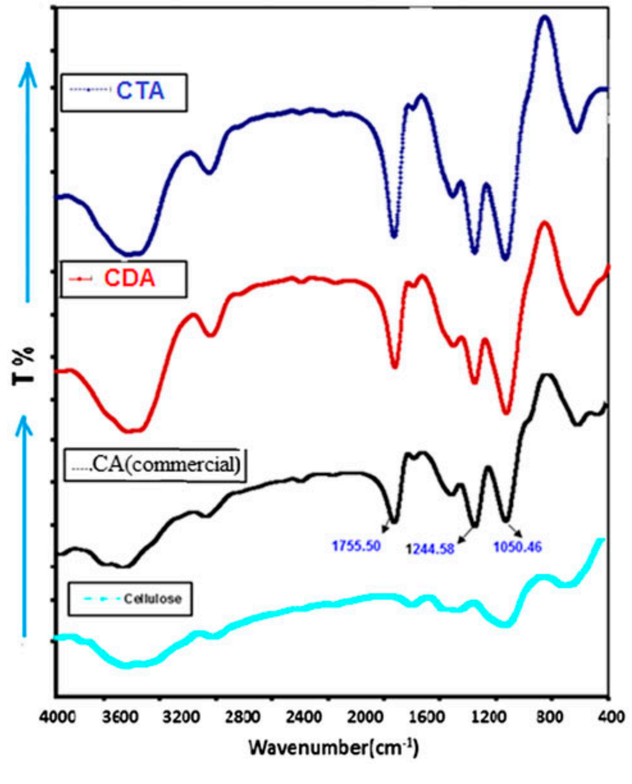

Fig. 6. FTIR spectra of cellulose, commercial CA, CDA, and CTA.

the –C–O–C single bond of the cellulosic esters. A peak at 741 cm^{-1} is assigned to C–H bending vibration of cellulose [9]. The formation of CTA and CDA is confirmed by the appearance of the band at 1,755 cm^{-1} of C=O of the carboxylic groups due to the presence of the acetyl group. The peak intensities of the acetate group at 1,755 cm^{-1} indicate the DS of cellulose acetate. As the DS increases, the absorption intensity of this peak increases [17,18].

3.4. Solubility of CDA and CTA

The solubility test was performed to differentiate between CDA and CTA. CDA is soluble in acetone while CTA is not. The opposite is true for chloroform. A mixture of chloroform and methanol dissolves both CDA and CTA. These results are presented in Table 1. One hydroxyl group present in CDA has increased the solubility in acetone while the CTA had no hydroxyl groups [14].

3.5. XRD of CDA and CTA

The XRD patterns in the range of 5°–45° for four different CA materials are shown in Fig. 7. It is found that the amorphous broad peak area of the commercial CA material was significantly larger than that of CTA and CDA. For the reference CA material, the 2θ angle is ranged from 5° to 24° and there were three small peaks at 7°, 13°, and 15°. In addition, one main diffused peak appeared at 22°. The commercial CA material is composed of crystalline and amorphous regions, where the broad peak at 20° suggests that this material possesses mainly amorphous structure [19,20]. The XRD patterns of CDA and CTA appeared to be highly resolved when compared with that of CA. The three diffraction peaks in the range of 8°–14° and the principal peak at 22.4° for CDA show higher intensities than those of CTA and CA [21]. The diffraction peaks at 15.5° and 22.4° are sharper and narrower in the XRD patterns of CTA and CDA indicating that the acetylation process increases the degree of crystallinity of the polymer chains. The XRD patterns show identical characteristic peaks in CDA and CTA around 7.07°, 16.1°, and 22.4° that appear but with a small change in the peak intensity, which increase with the decrease in the acetylation [22].

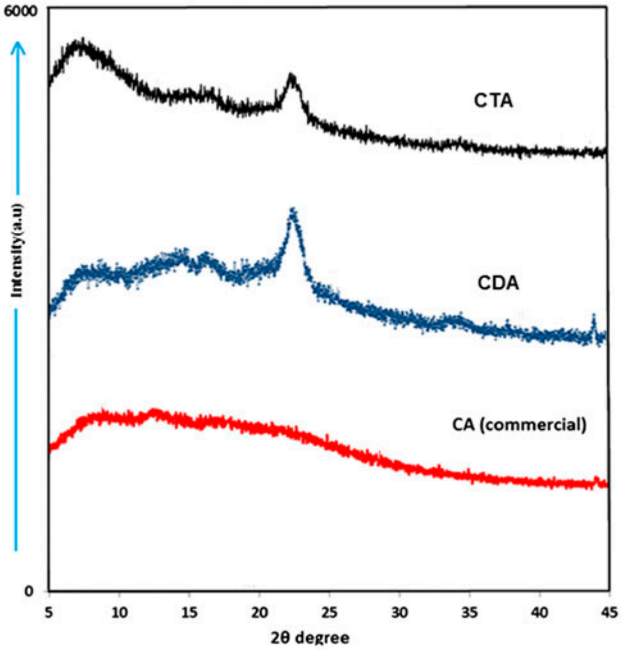

Fig. 7. XRD patterns of commercial CA membrane, and membranes made of CDA and CTA prepared from rice straw.

3.6. TGA of CDA and CTA

In general, the thermal stability and the thermal properties depend on the structure and bonding within the material. The thermal stability of CA of different sources was examined. The thermal gravimetric, TG, curves of the prepared cellulose and the reference (commercially available cellulose acetates) are shown in Fig. 8. The degradation of cellulose and cellulose acetate occurs in three stages. In the first stage, from 25 to ~75°C, a slight loss in weight (about 5%) took place as the volatilization of the volatile matter and

Table 1
Solubility results for the CTA and CDA

Solvent	Type CA	
	CTA	CDA
Acetone	Insoluble	Soluble
Chloroform	Soluble	Insoluble
Mixture of chloroform and methanol (1:1)	Soluble	Soluble

the evaporation of water were ejected and then the weight became stable up to 255˚C. The second stage started at ~255˚C and ended at ~403˚C, which represents the main decomposition process of the cellulose and cellulose acetate chains involving a rapid loss in weight. The total weight loss has reached a value between 75 and 85%. Once more, the weight became stable till 500˚C. The third stage started at 500˚C and ended at ~598˚C, indicating the carbonization of the degraded products into ash. Although the cellulose acetate and their substituted compounds showed a similar pattern of degradation, the CDA showed slightly more stability in comparison to other compounds. Such relative stability may be attributed to the presence of the OH and the formation of intermolecular hydrogen bonding. The relative stability among the different CDA of different sources may be attributed to the varying degrees of acetylation [23].

3.7. Morphological properties of CA-RO membranes

Fig. 9 presents the SEM images of surface, bottom, and cross section of the CA-RO membranes with and without annealing. The micrographs of the CA-RO membranes without annealing process show that the top surface is smooth and dense with no cracks. SEM micrographs of the bottom surface show large number of pores which proves the asymmetric structure of the prepared membranes [5]. SEM images of the CA-RO membranes after annealing reveal an asymmetric structure shown in the cross section with ridge-and-valley in the top layer and macrovoid structures in the support layer which indicate instantaneous demixing as the overall mechanism of polymer solidification. The cross-sectional images of the membranes that illustrate the macrovoids grew after annealing [24].

Two- and three-dimensional AFM images of pure CA and CA-RO membranes are depicted in Fig. 10.

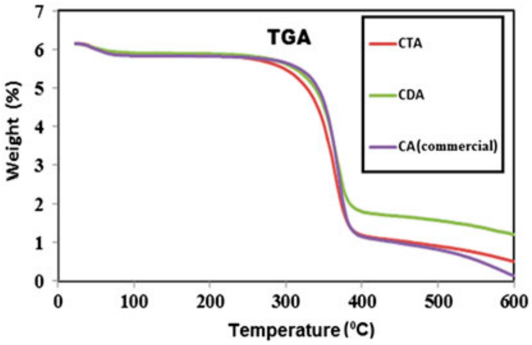

Fig. 8. TGA curves of commercial CA, CDA, and CTA prepared from rice straw.

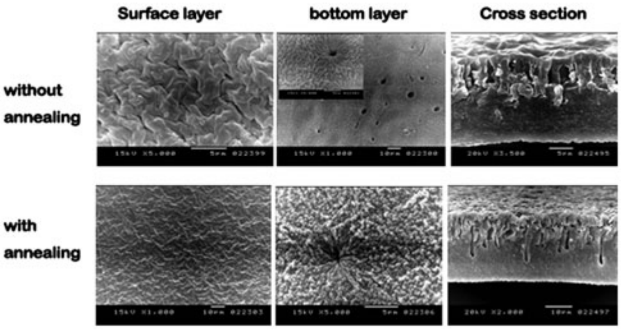

Fig. 9. SEM images of CA-RO membranes before and after annealing.

Analysis of AFM images revealed the roughness of the membrane surface as measured from the arithmetic mean roughness value (Fig. 10(b)). Roughness of the membrane surface is attributed to the presence of “hills and valleys”, which increases the surface area and hence provides more binding sites. The pristine CA-RO membrane displays a surface roughness of Ra = 202 nm. Fouling is often linked to the intrinsic membrane properties which indicate that fouling rates increase with membrane surface roughness because foulant particles are more likely to be entrained by rougher topologies than by smoother membrane surfaces [25].

3.8. Effect of annealing on the hydrophilic properties of CA-RO membranes

CA membranes have remarkable hydrophilic properties due to the three active hydroxyls in each repeating unit of cellulose molecule. It is found that the contact angles for CA-RO membranes before and after annealing were (66.4 ± 2.8) and (58.5 ± 1.8), respectively. The improvement in the CA-RO membrane surface of the hydrophobicity after annealing is attributed to an increase in the average size of the hydrophilic clusters. Annealing helps the polymer segments to be rearranged in a more ordered structure and therefore, the crystalline regions become more enhanced than the amorphous ones. The changes in diffusivity are brought about by the changes in the polymer structure or free volume [26].

3.9. Effect of annealing on the rejection and flux of the RO–CA membranes

Fig. 10 displays the salt rejection and water flux vs. the operating pressure of CA-RO membranes without annealing. It is observed that the values of water flux

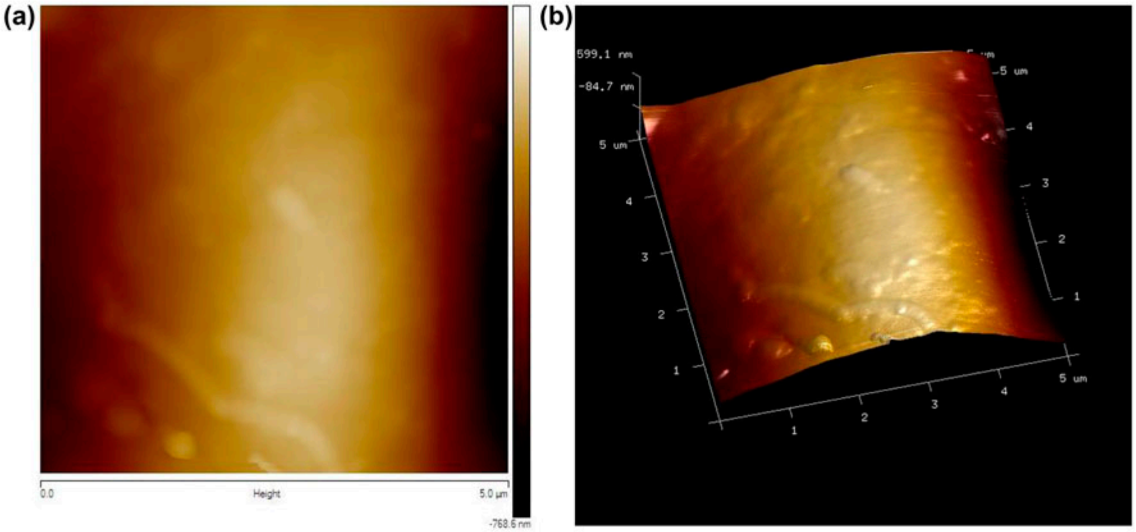

Fig. 10. 2D (a) and 3D (b) AFM images of CA-RO membranes.

and salt rejection are 7.1 L/m^2 h and 87.4%, respectively, at 16 bar. The effect of the annealing process on the flux and rejection of the CA-RO membranes is illustrated in Fig. 11. The trends in Fig. 12 indicate that post-treatment via thermal annealing at 85˚C for 10 min reduces the water flux and increases the salt rejection. It is observed that the flux becomes 4.76 L/m^2 h and the salt rejection is 93.3% at 14 bar. Rearrangement of the polymer segments would only occur where the polymer chains were close enough to change from intramolecular hydrogen bonding of molecules to intermolecular hydrogen bonding, namely in the dense active layer due to the small but significant loss in pore volume in the support layer. This is attributed to either the collapse of larger pores or for not being formed in the first place. At higher pressures, the corresponding high fluxes may have led to concentration polarization in the measuring cell, thereby causing a drop in the salt retention [27,28].

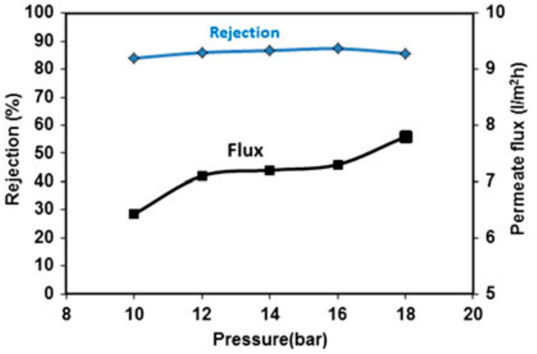

Fig. 11. Salt rejection and water flux vs. feed pressure of CA-RO membrane without annealing.

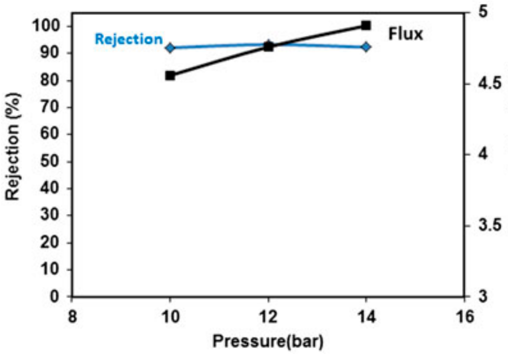

Fig. 12. Salt rejection and water flux vs. feed pressure of CA-RO membrane after annealing.

3.10. Salt rejection and water flux of grafted CA-RO membranes

Fig. 13 presents the salt rejection and water flux vs. grafting wt% of AMPSA onto CA-RO membranes that are prepared from rice straw. The CA-RO membrane grafted with 15 wt% AMPSA has the rejection of 93.5% and 8.3 L/m^2 h water fluxes. At a high grafting weight percentage of 20, the operating pressure has increased to 14 bar to produce a salt rejection of only 77.8% and 8.2 L/m^2 h water fluxes. This is due to the higher thickness of the top dense layer at higher weight percentage of grafting; the number of pores

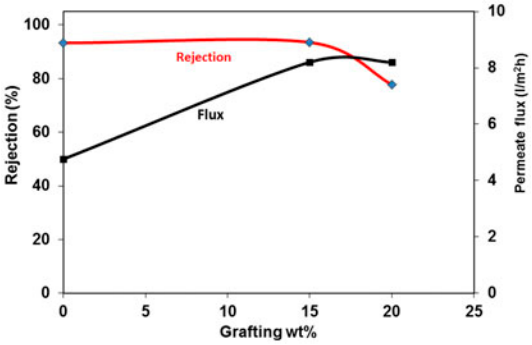

Fig. 13. Salt rejection and water flux vs. grafting wt% of AMPSA onto CA-RO membranes prepared from rice straw.

has decreased and consequently, the salt rejection has been reduced and the operating pressure has increased.

4. Conclusion

We have succeeded to prepare CDA and CTA from rice straw with a yield of 50 wt% and produced CA-RO membranes using the phase inversion technique. It was found that the CTA prepared from rice straw has a DS of 2.8 and 1.75 for CDA. SEM images of CA-RO membranes after annealing revealed asymmetric ridge-and-valley structure on the top layer and macrovoid structures in the support layer. The hydrophilicity of the CA-RO membranes was slightly enhanced by the annealing process, where the contact angles were decreased from 66.4 to 58.5 before and after the annealing process. It was observed that the value of water flux was 4.76 L/m^2 h and salt rejection was 93.3% for the annealed CA-RO membrane. The CA-RO membrane grafted with 15 wt% AMPSA has a rejection value of 93.5% and water fluxes of 8.3 L/m^2 h.

Acknowledgments

The authors acknowledge the Science and Technology Development Fund in Egypt for supporting this project (project ID 3988).

References

[1] X. Rodríguez, Y. Elasraag, Assessing the total factor productivity of cotton production in Egypt, J. Plos one 27 (2015) 1–14.

[2] P. Kulpinski, A. Erdman, M. Namyslak, J. Fidelus, Cellulose fibers modified by Eu^{3+}-doped yttria-stabilized zirconia nanoparticles, Cellulose 19 (2012) 1259–1269.

[3] K. Buzała, P. Przybysz, J. Rosicka-Kaczmarek, H. Kalinowska, Production of glucose-rich enzymatic hydrolysates from cellulosic pulps, Cellulose 22 (2015) 663–674.

[4] J. He, M. Zhang, S. Cui, S. Wang, High-quality cellulose triacetate prepared from bamboo dissolving pulp, J. Appl. Polym. Sci. 113 (2009) 456–465.

[5] B. Atanu, C. Badal, W. John, R. Shogren, V. Willett, Process for obtaining cellulose acetate from agricultural by-products, Carbohydr. Polym. 64 (2006) 134–137.

[6] A. Muhammed, E. Hashash, G. Mekewi, Polyvinyl alcohol-cellulose acetate composite reverses osmosis membranes: I. Synthesis and characterization, Hydrol. Curr. Res. 3 (2012) 1–7.

[7] V. Scott, M. Cray, V. Vilker, K. Nobe, Reverse osmosis cellulose acetate membranes II. Dependence of transport properties on acetyl content, J. Membr. Sci. 59 (1991) 317–330.

[8] W. Ho, K. Sirkar, Membrane Handbook, in: W. Winston (Ed.), Chapman & Hall, New York, NY, 1992, pp. 263–355.

[9] H. Myeong-Jin, B. Dibakar, Thermal annealing effect on cellulose acetate reverse osmosis membrane structure, Desalination 101 (1995) 195–200.

[10] W. Blau, R. Padamati, A. Drury, A membrane and use thereof, European Patent, EP 2 305 368 A1, (2011).

[11] U. Akpabio, I. Effiong, A. Akpakpan, Preparation of pulp and cellulose acetate from nypa palm leaves, Int. Environ. Bioenergy 3 (2012) 179–194.

[12] Y. Cao, J. Wu, T. Meng, J. Zhang, J. He, H. Li, Y. Zhang, Acetone-soluble cellulose acetates prepared by one-step homogeneous acetylation of cornhusk cellulose in an ionic liquid 1-allyl-3-methylimidazolium chloride (AmimCl), Carbohydr. Polym. 69 (2007) 665–672.

[13] S. Loeb, S. Sourirajan, Sea Water demineralization by means of an osmotic membrane, Adv. Chem. Ser. 38 (1963) 117–132.

[14] C. Fritzmann, J. Löwenberg, T. Wintgens, T. Melin, State of the art of reverse osmosis desalination, Desalination 216 (2007) 1–76.

[15] V. Miyamoto, Y. Sato, T. Shibata, H. Inagaki, Nuclear magnetic resonance studies of cellulose acetate, J. Polym. Sci. 22 (1984) 2363–2370.

[16] H. Kono, Chemical shift assignment of the complicated monomers comprising cellulose acetate by two-dimensional NMR spectroscopy, Carbohydr. Res. 375 (2013) 136–144.

[17] J. Li, L.-P. Zhang, F. Peng, J. Bian, T.-Q. Yuan, F. Xu, R.-C. Sun, Microwave-assisted solvent-free acetylation of cellulose with acetic anhydride in the presence of iodine as a catalyst, Molecules 14 (2009) 3551–3566.

[18] B. Tosh, Thermal analysis of cellulose esters prepared from different molecular weight fractions of high a-cellulose pulp, Indian, J. Chem. Technol. 18 (2011) 451–457.

[19] M. Gopiraman, K. Fujimori, K. Zeeshan, B. Kim, I. Kim, Structural and mechanical properties of cellulose acetate/graphene hybrid nanofibers: Spectroscopic investigations, Express Polym. Lett. 7 (2013) 554–563.

[20] S. Wu, X. Qin, M. Li, The structure and properties of cellulose acetate materials: A comparative study on electrospun membranes and casted films, J. Ind. Text. 44 (2014) 85–98.

[21] G. Fan, M. Wang, C. Liao, T. Fang, J. Li, R. Zhou, Isolation of cellulose from rice straw and its conversion into cellulose acetate catalyzed by phosphotungstic acid, Carbohydr. Polym. 94 (2013) 71–76.

[22] G. Arthanareeswaran, P. Thanikaivelan, K. Srinivasn, D. Mohan, M. Rajendran, Synthesis characterization and thermal studies on cellulose acetate membranes with additive, Eur. Polym. J. 40 (2004) 2153–2159.

[23] H. Kawakami, M. Mikawa, S. Nagaoka, Gas transport properties in thermally cured aromatic polyimide membranes, J. Membr. Sci. 118 (1996) 223–230.

[24] E. Jesse, W. Douglas, F. Steven, D. Kent, The effects of thermal annealing on commercial nafion membranes, J. Membr. Sci. 298 (2007) 190–201.

[25] S. Azari, L. Zou, E. Cornelissen, Y. Mukai, Facile fouling resistant surface modification of microfiltration cellulose acetate membranes by using amino acid I-DOPA, Water Sci. Technol. 68 (2013) 901–905.

[26] M.A. Mohammad, B. Dariush, K. Ali, T. Meisam, Characterization of polymeric membranes for membrane distillation using atomic force microscopy, Desalin. Water Treat. 51 (2013) 31–33.

[27] O.V. Loreen, S.A. Tabatabai, N. Dhaka, Algal blooms: An emerging threat to seawater reverse osmosis desalination, Desalin. Water Treat. 2 (2014) 1–11.

[28] M. Ulbricht, R.M. Malaisamy, Insights into the mechanism of molecular imprinting by immersion precipitation phase inversion of polymer blends via a detailed morphology analysis of porous membranes, J. Mater. Chem. 15 (2005) 1487–1497.